RESEARCH ARTICLE

Check for updates

A new twist on an old ligand: a [Mn₁₆] double square wheel and a [Mn₁₀] contorted wheel†

Thomais G. Tziotzi,[a] Marco Coletta, [iD][b] Mark Gray,[b] Cameron L. Campbell,[c]
Scott J. Dalgarno, [iD][c] Giulia Lorusso, [iD][d] Marco Evangelisti, [iD][d]
Euan K. Brechin [iD] *[b] and Constantinos J. Milios [iD] *[a]

Ligand design remains key to the synthesis of coordination compounds possessing specific topologies, nuclearities and symmetries that direct targeted physical properties. N,O-chelates based on ethanolamine have been particularly prolific in constructing a variety of paramagnetic 3d transition metal complexes with fascinating magnetic properties. Here, we show that combining three ethanolamine moieties within the same organic framework in the form of the pro-ligand 1,3,5-tri(2-hydroxyethyl)-1,3,5-triazacyclohexane (LH₃) leads to the formation of two highly unusual Mn wheels. Reaction of Mn(NO₃)₂·6H₂O with LH₃ in basic methanolic solutions leads to the formation of [Mn$_{12}^{III}$Mn$_4^{II}$(μ₃-O)₆(μ-OH)₄(μ₃-OMe)₂(μ-OMe)₂(L)₄(LH)₂(H₂O)₁₀](NO₃)₆(OH)₂ (**1**) and [Mn$_{10}^{III}$(μ₃-O)₄(μ-OH)₄(μ-OMe)₄(L)₄(H₂O)₄](NO₃)₂ (**2**), the only difference in the synthesis being the ratio of metal:ligand employed. The structure of the former describes two offset [Mn$_6^{III}$Mn$_2^{II}$] square wheels, linked through a common centre, and the latter a single [Mn$_{10}^{III}$] wheel twisted at its centre, such that the top half is orientated perpendicular to the bottom half. In both cases the L³⁻/LH²⁻ ligands dictate the orientation of the Jahn–Teller axes of the Mnᴵᴵᴵ ions which lie perpendicular to the triazacyclohexane plane. Direct current magnetic susceptibility and magnetisation data reveal the presence of competing exchange interactions in **1** and strong antiferromagnetic interactions in **2**. Given the simplicity of the reactions employed and the paucity of previous work, the formation of these two compounds suggests that LH₃ will prove to be a profitable ligand for the synthesis of a multitude of novel 3d transition metal complexes.

Introduction

The development of magneto-structural relationships in molecular coordination compounds can be traced back to measurements of copper(ɪɪ) acetate and the basic metal(ɪɪɪ) carboxylates, wherefrom their dinuclear and trinuclear structures, solved later, were predicted.[1,2] Detailed, quantitative analyses of a variety of di-, tri- and tetranuclear 3d transition metal complexes followed, often revealing a complex relationship between exchange interactions/magnetic anisotropy, and the identity of the ligand, metal-metal distances, metal-ligand

bond lengths, bond angles, torsions angles, and metal geometry – correlations now benefitting from detailed theoretical input.[3–5] Interest in the magnetochemistry of Mn compounds in particular was boosted by the discovery of single-molecule magnets (SMMs), the first of which was a [Mn₁₂] complex[6] whose structure was reported some years earlier.[7] Magneto-structural studies were aided and abetted by magnetic measurements on the large library of low-nuclearity Mn compounds initially established as metalloenzyme model complexes, particularly those pertaining to the water oxidation centre in PSII.[8] These proved vital in both the development of novel synthetic methodologies for the construction of new Mn compounds whose nuclearities now reach eighty four[9] and in understanding the origin of the slow magnetisation relaxation dynamics.[10]

Central to these studies has been the design of ligands capable of bridging between paramagnetic metal ions in a particular manner, be that within a rigid or flexible framework. One very successful class of ligands in the latter category are N,O-chelates including 2-(hydroxymethyl)pyridine (hmpH),[11] 2,6-pyridinemethanol (pdmH₂),[12] di- (R-deaH₂)[13] and tri-ethanolamine (teaH₃)[14] which are all characterised by posses-

[a]*Department of Chemistry, The University of Crete, Voutes, 71003 Herakleion, Greece. E-mail: komil@uoc.gr*
[b]*EaStCHEM School of Chemistry, The University of Edinburgh, David Brewster Road, Edinburgh, Scotland, EH9 3FJ, UK. E-mail: E.Brechin@ed.ac.uk*
[c]*Institute of Chemical Sciences, Heriot-Watt University, Riccarton, Edinburgh, Scotland, EH14 4AS, UK*
[d]*Instituto de Nanociencia y Materiales de Aragón (INMA), CSIC – Universidad de Zaragoza, 50009 Zaragoza, Spain*
†Electronic supplementary information (ESI) available: FTIR-ATR spectra (Fig. S1), PXRD patterns (Fig. S2), coordination modes of the ligand (Fig. S3), BVS calculations (Tables S1 and S2). See DOI: 10.1039/d0qi01495h
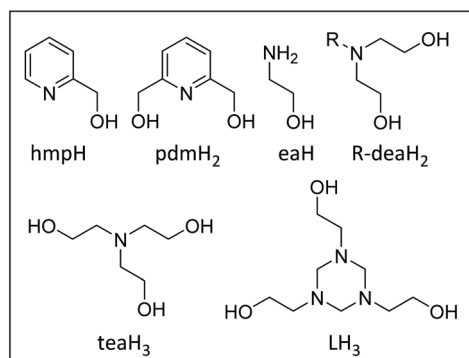
1804 | *Inorg. Chem. Front.*, 2021, **8**, 1804–1809

This journal is © the Partner Organisations 2021

Fig. 1 The N,O-chelates 2-(hydroxymethyl)pyridine (hmpH), 2,6-pyridinedimethanol (pdmH$_2$), di- (R-deaH$_2$) and triethanolamine (teaH$_3$), and 1,3,5-tri(2-hydroxyethyl)-1,3,5-triazacyclohexane (LH$_3$), all of which contain one or more linked ethanolamine (eaH) moieties.

sing one or more linked ethanolamine (eaH)[15] moieties (Fig. 1). Herein we extend this body of work to include the pro-ligand 1,3,5-tri(2-hydroxyethyl)-1,3,5-triazacyclohexane (LH$_3$), which contains three linked eaH units. A search of the Cambridge Structural Database (CSD) reveals just two hits in 3d transition metal chemistry. The first,[16] in 1999, was the monomer [Cr(CO)$_3$(LH$_3$)] and the second, in 2019, an aesthetically pleasing torus-like [Mn$_{16}$] complex, [Mn$_2^{II}$Mn$_{14}^{III}$(trz)$_{14}$L$_4$(μ$_3$-O)$_8$(H$_2$O)$_{10}$](ClO$_4$)$_6$ (Htzr = 1,2,3-triazole), in which the ligand was generated serendipitously *in situ*, upon the reaction of (2-hydroxymethyl)-1,2,3-triazole and 2-aminoethanol in the presence of manganese perchlorate.[17]

Experimental

General methods

All chemicals were obtained from commercial suppliers (Sigma-Aldrich) and were used without further purification/treatment.

Synthesis

LH$_3$ was prepared as previously described.[16]

[Mn$_{12}^{III}$Mn$_4^{II}$(μ$_3$-O)$_6$(μ-OH)$_4$(μ$_3$-OMe)$_2$(μ-OMe)$_2$(L)$_4$(LH)$_2$(H$_2$O)$_{10}$]-(NO$_3$)$_6$(OH)$_2$ (**1**). Mn(NO$_3$)$_2$·6H$_2$O (143.5 mg, 0.5 mmol) and LH$_3$ (103.58 mg, 0.5 mmol) were stirred in MeOH for 30 minutes in the presence of NEt$_3$ (1 mmol). The solution was then filtered and allowed to stand. Crystals of **1** formed in ~5 days in a yield of 20%. Elemental analysis (%) calcd for C$_{62}$H$_{178}$N$_{24}$O$_{76}$ (**1**): C 22.82, H 4.89, N 11.01; found: C 22.93, H 4.71, N 11.13.

[Mn$_{10}^{III}$(μ$_3$-O)$_4$(μ-OH)$_4$(μ-OMe)$_4$(L)$_4$(H$_2$O)$_4$](NO$_3$)$_2$ (**2**). Mn(NO$_3$)$_2$·6H$_2$O (143.5 mg, 0.5 mmol) and LH$_3$ (207.16 mg, 1.00 mmol) were stirred in MeOH for 30 minutes in the presence of NEt$_3$ (1 mmol). The solution was then filtered and allowed to stand. Crystals of **2** formed in ~3 days in a yield of 25%. Elemental analysis (%) calcd for C$_{40}$H$_{96}$Mn$_{10}$N$_{14}$O$_{34}$ (**2**): C 25.74, H 5.18, N 10.51; found: C 25.62, H 5.06, N 10.42.

Crystallography

Using Olex2,[18] the structures were solved with the SHELXT[19] structure solution program using Intrinsic Phasing and refined with the SHELXL[20] refinement package using Least Squares minimisation. Crystal data for **1** (CCDC 2042257†): C$_{58}$H$_{148}$Mn$_{16}$N$_{24}$O$_{62}$ (M = 3053.04 g mol^{-1}), monoclinic, space group $P2_1/n$ (no. 14), a = 15.3417(7) Å, b = 22.1812(11) Å, c = 18.9436(8) Å, β = 92.046(2)°, V = 6442.3(5) Å^3, Z = 2, T = 200.0 K, Bruker Apex II diffractometer, μ(CuKα) = 13.098 mm^{-1}, D_{calc} = 1.574 g cm^{-3}, 160 106 reflections measured (6.138° ≤ 2Θ ≤ 131.672°), 11 061 unique (R_{int} = 0.0991, R_{sigma} = 0.0384) which were used in all calculations. The final R_1 was 0.0743 ($I > 2\sigma(I)$) and wR_2 was 0.2285 (all data). Crystal data for **2** (CCDC 2042258†): C$_{40}$H$_{96}$Mn$_{10}$N$_{14}$O$_{34}$ (M = 1866.70 g mol^{-1}), tetragonal, space group $I4_1/a$ (no. 88), a = 18.2751(8) Å, c = 32.445(3) Å, V = 10 836.1(13) Å^3, Z = 4, T = 100.0 K, Bruker D8 Venture diffractometer, μ(CuKα) = 9.687 mm^{-1}, D_{calc} = 1.144 g cm^{-3}, 182 310 reflections measured (8.748° ≤ 2Θ ≤ 149.676°), 5547 unique (R_{int} = 0.0634, R_{sigma} = 0.0144) which were used in all calculations. The final R_1 was 0.0297 ($I > 2\sigma(I)$) and wR_2 was 0.0927 (all data). Neighbouring clusters in the structure of **2** pack so as to form large solvent/anion occupied spaces that are extremely disordered as evidenced by the presence of diffuse electron density. The presence of nitrate counterions in the large voids in the structure of **2** was confirmed by IR spectroscopy. Given the diffuse nature of the density in the difference map it is not possible (or sensible) to try and model this.

Magnetometry

Variable-temperature and variable-field magnetic measurements were carried out using a MPMS-XL Quantum Design magnetometer equipped with a 5 T magnet. Diamagnetic corrections were applied using Pascal's constants.

Powder-XRD measurements

Powder XRD measurements were collected on freshly prepared samples of the complexes on a PANanalytical X'Pert Pro MPD diffractometer.

Infra-red spectroscopy

FTIR–ATR (Fourier-transform infrared–attenuated total reflectance) spectra were recorded on a PerkinElmer FTIR Spectrum BX spectrometer.

Results and discussion

The 1:1 reaction of LH$_3$ with Mn(NO$_3$)$_2$·6H$_2$O in a basic MeOH solution produces dark brown crystals of [Mn$_{12}^{III}$Mn$_4^{II}$(μ$_3$-O)$_6$(μ-OH)$_4$(μ$_3$-OMe)$_2$(μ-OMe)$_2$(L)$_4$(LH)$_2$(H$_2$O)$_{10}$](NO$_3$)$_6$(OH)$_2$ (**1**; Fig. 2) after 5 days. **1** crystallises in a monoclinic cell and structure solution was performed in the space group $P2_1/n$. The asymmetric unit of **1** contains half the cluster complex and three nitrate/one hydroxide counter ions. The metallic skeleton of the asymmetric unit contains a non-planar, asymmetric
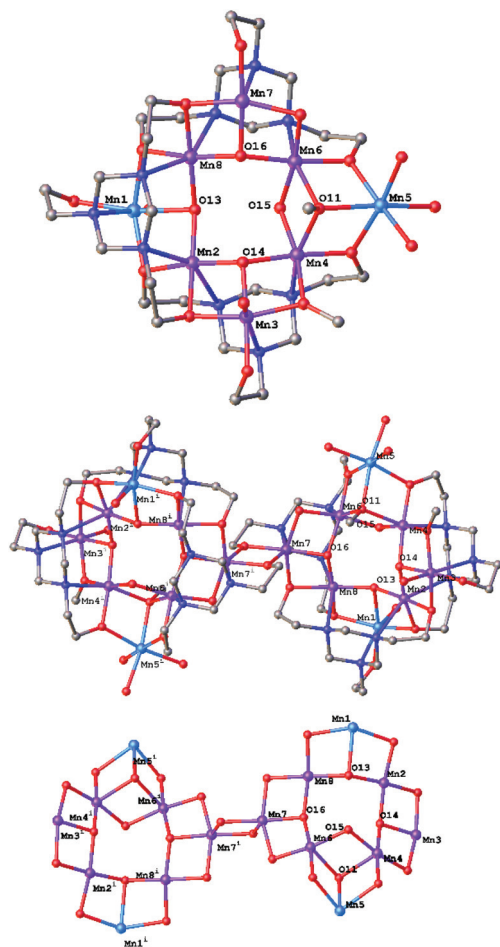
This journal is © the Partner Organisations 2021

Inorg. Chem. Front., 2021, **8**, 1804–1809 | **1805**

Fig. 2 The asymmetric unit found in **1** (top) and its symmetry expanded structure (middle). The metallic core of **1**, showing the connection of the two {Mn$_8$} units (bottom). Colour code: Mn^{III} = purple, Mn^{II} = light blue, O = red, N = blue, C = grey. H-atoms and counter anions have been omitted for clarity.

[Mn$_6^{III}$Mn$_2^{II}$] square wheel (Fig. 2, top) of corner sharing [Mn$_3^{III}$] (Mn2–Mn4, Mn6–Mn8) and [Mn$_2^{III}$Mn^{II}] triangles in which the two Mn^{II} ions (Mn1, Mn5) are opposed. The three μ$_3$-O^{2-} ions (O13, O14, O16) occupy three of the four positions on the inside of the square wheel (Mn2, Mn4, Mn6, Mn8) further bridging to Mn^{III} ions (Mn3, Mn7) or a Mn^{II} ion (Mn1) in the [Mn$_3^{III}$] and [Mn$_2^{III}$Mn^{II}] triangles, respectively. The fourth side of the inner wheel (Mn4, Mn6) is occupied by a μ-OH$^-$ ion (O15) which is H-bonded to O13 (O⋯O, 2.806 Å). This does not bridge to the third Mn ion in its triangle, this job being performed by the sole μ$_3$-MeO$^-$ ion (O11) present. The remaining μ-OH/OMe ions bridge between neighbouring Mn^{III} ions around the outside of the wheel (Mn3–O9(H)–Mn3, Mn6–O12(H)–Mn7, Mn3–O10(Me)–Mn4). The three 1,3,5-tri(2-hydroxyethyl)-1,3,5-triazacyclohexane ligands are of two types, two are fully deprotonated (L^{3-}) and one is doubly deprotonated (LH^{2-}). One μ$_5$-bridging L^{3-} ion directs the formation of a [Mn$_3^{III}$] triangle (Mn2–4) through N,O-chelation, with two of its three O-atoms (O1, O3) further bridging to the neighbouring

Mn^{II} ions. The third O-atom (O2) remains terminally co-ordinated. The second μ$_6$-L^{3-} ion bridges in a similar fashion, but with the third O-atom now bridging between the two [Mn$_8$] wheels (Fig. 2, middle). The μ$_5$-LH^{2-} ligand N,O-chelates to the Mn ions in the 'lower' [Mn$_2^{III}$Mn^{II}] triangle (Mn1, Mn2, Mn8). The deprotonated O-atoms further bridge to neighbouring Mn^{III} ions, while the protonated arm remains terminally co-ordinated to Mn1. The Mn^{III} ions are all six-coordinate and in Jahn-Teller (JT) distorted octahedral geometries. In each case the JT axis is directed by the Mn–N(L) bonds. The coordination of Mn3 is completed with a single H$_2$O molecule. The Mn^{II} ions are also six coordinate and in regular octahedral geometries, with Mn1 having one and Mn5 having three coordinated H$_2$O molecules.

There are several short intermolecular interactions. The H$_2$O molecule (O0) and terminally bonded O(L) atom (O2) on Mn3 are H-bonded to their symmetry equivalent atoms on neighbouring molecules (O⋯O, ~2.63 Å) creating 1D chains of wheels down the *c*-axis of the crystal. (O0) is also H-bonded to a NO$_3^-$ counter anion (O0⋯O20, ~2.86 Å) which is further H-bonded to both H$_2$O solvent of crystallisation (O21⋯O31, ~2.80 Å) and to the H$_2$O molecule (O22⋯O29, ~2.63 Å) and terminal O(L) on Mn1 (O7⋯O21, ~2.75 Å). The NO$_3^-$ counter anions are also H-bonded to the H$_2$O molecules on Mn5 (O17⋯O25, ~2.78 Å; O18⋯O23, ~2.72 Å; O19⋯O27, ~2.87 Å) and the μ-OH$^-$ ion bridging between Mn6–Mn7. The result is a complicated network of interactions in all three dimensions.

Repeating the reaction that produces **1**, but increasing the Mn : LH$_3$ ratio to 1 : 2 produces the complex [Mn$_{10}^{III}$(μ$_3$-O)$_4$(μ-OH)$_4$(μ-OMe)$_4$(L)$_4$(H$_2$O)$_4$](NO$_3$)$_2$ (**2**). **2** crystallises in the tetragonal space group $I4_1/a$ (Fig. 3, top) with three Mn^{III} ions, one O^{2-} (O5), one OMe$^-$ (O4) and one OH$^-$ (O7) ion in the assymetric unit. The metallic skeleton of **2** describes a rather contorted [Mn$_{10}^{III}$] square wheel of corner sharing [Mn$_3^{III}$O] triangles, twisted at its centre such that the top half is orientated perpendicular to the bottom half (Fig. 3, bottom). There are two corner sharing [Mn$_3^{III}$O] triangles in each [Mn$_5$] half, each with a μ$_3$-O^{2-} at its centre and a μ-OMe$^-$ along the Mn1–Mn3 edge (Mn1–O4–Mn3, 96.9°). The two halves of the molecule are connected *via* four μ-OH$^-$ ions (Mn01–O7–Mn01, ~138°), which are H-bonded to the μ$_3$-O^{2-} ions (O7⋯O5, 2.895 Å). There are two L^{3-} ligands in each [Mn$_5$] half of the molecule bonding in an identical μ$_4$-fashion, N,O-chelating to the Mn^{III} ions with just one of the three arms (O2) further bridging to a neighbouring metal centre. The Mn^{III} ions are all in JT distorted octahedral geometries, again dictated by the Mn–N(L) bonds. The remaining coordination site on Mn1 is occupied by a H$_2$O molecule (O6) which, alongside O1(L), H-bond to the symmetry equivalent atoms on neighbouring molecules (O6⋯O1, 2.588 Å). The result is that the [Mn$_{10}$] clusters pack in an aesthetically pleasing brickwork-like fashion, forming large solvent filled channels (Fig. 4). O6 also forms an internal H-bond to one of the terminally bonded O(L) atoms (O6⋯O3, 2.579 Å).

There are several structural similarities between **1** and **2**. Both are square wheels composed of corner-sharing [Mn$_3$O]$^{n+}$

1806 | *Inorg. Chem. Front.*, 2021, **8**, 1804–1809

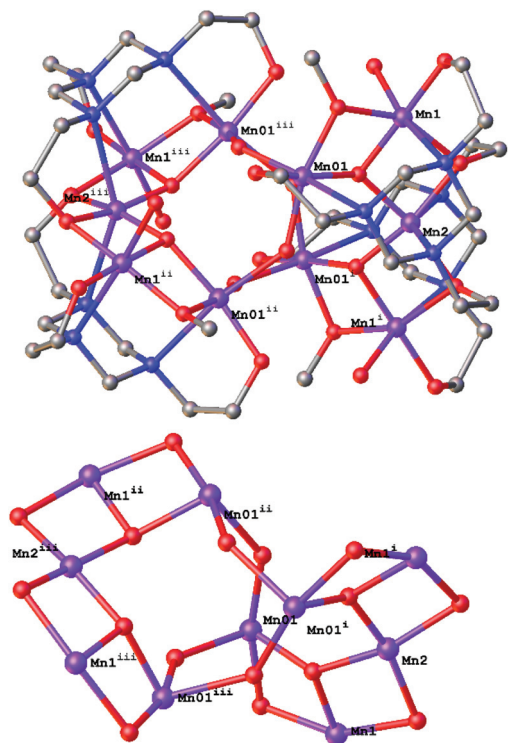This journal is © the Partner Organisations 2021

Fig. 3 The crystal structure of **2** (top) and its metallic core (bottom). Colour code: Mn^{III} = purple, O = red, N = blue, C = grey. H-atoms and counter anions have been omitted for clarity.
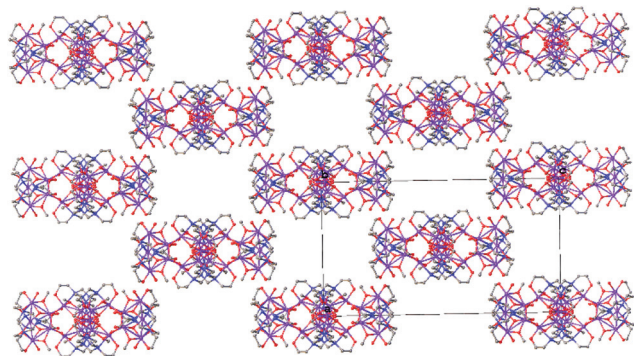

Fig. 4 The brickwall-like crystal packing of **2** in the *ac* plane. Colour code: Mn^{III} = purple, O = red, N = blue, C = grey. H-atoms and counter anions have been omitted for clarity.

triangles as directed by the L^{3-} and LH^{2-} ligands. The N-atoms of the ligands also dictate the orientation of the JT axes (and hence the d$_{z^2}$ orbital) of the Mn^{III} ions, which has important design consequences for tuning magnetic exchange and magnetic anisotropy.[21] Both compounds possess terminally bonded H$_2$O molecules which mediate similar intermolecular interactions in the extended structure. Perhaps the biggest differences between the two compounds, despite the very similar synthetic procedures, is the high symmetry of **2** *versus* the asymmetry of **1**, and the dimerization of wheels in **1**

versus the single wheel in **2**. The intricacies involved in driving these differences are unknown and will require a larger library of clusters to be synthesised and characterised. Given that **1** and **2** are just the second and third Mn complexes made with LH$_3$, it would seem likely that many more species await discovery. It also suggests that other homo- and heterometallic 3d and 4f cluster compounds will be readily accessible. A search of the Cambridge structural database reveals that, bar [Mn$_2^{II}$Mn$_{14}^{III}$(trz)$_{14}$L$_4$(μ_3-O)$_8$(H$_2$O)$_{10}$](ClO$_4$)$_6$, there are no [Mn$_{16}$] or [Mn$_{10}$] molecules in the literature with similar topologies to **1** and **2**.

Magnetic properties

The direct current (dc) molar magnetic susceptibility, χ, of freshly prepared polycrystalline samples of **1** and **2** were measured in an applied field, *B*, of 0.1 T, over the 2–300 K temperature, *T*, range. The purity of the samples was verified by means of PXRD comparison with the simulated data from the single-crystal structure (Fig. S3†). The experimental results are showed in Fig. 5, in the form of the χT product, where $\chi = M/B$, and *M* is the magnetisation of the sample. At room temperature the χT products of **1** (36.0 cm^3 K mol^{-1}) and **2** (15.4 cm^3 K mol^{-1}) are lower than the sum of the Curie constants expected for non-interacting [Mn$_{12}^{III}$Mn$_4^{II}$] (53.5 cm^3 K mol^{-1}) and [Mn$_{10}^{III}$] (30 cm^3 K mol^{-1}) units, respectively. As temperature decreases, the χT product for both complexes decreases rapidly and for **2** reaches a value close to 0 cm^3 K mol^{-1} at *T* = 2 K, clearly indicative of strong antiferromagnetic exchange and a diamagnetic ground state. For **1**, there is a plateau in the value of $\chi T \approx 24$ cm^3 K mol^{-1} between *T* = 15–25 K, before it decreases rapidly to a value of 10 cm^3 K mol^{-1} at *T* = 2 K. The plateau in χT is suggestive of the presence of competing ferro- and antiferromagnetic interactions which may, or may not, be related to the dimeric nature of the structure. Low-temperature variable-temperature-and-variable-field magnetisation data were measured in the temperature range 2–7 K, in magnetic fields up to 5.0 T (Fig. 6). At the lowest temperature and highest field measured, *M* reaches a
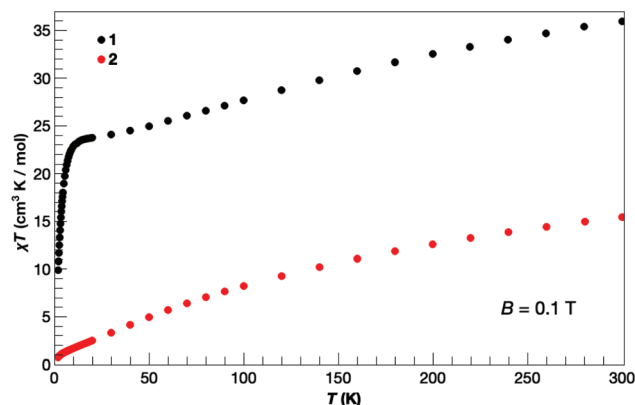

Fig. 5 Temperature dependence of the χT product, where χ is the dc molar magnetic susceptibility, for **1** and **2**, as labelled, collected for an applied magnetic field of *B* = 0.1 T.
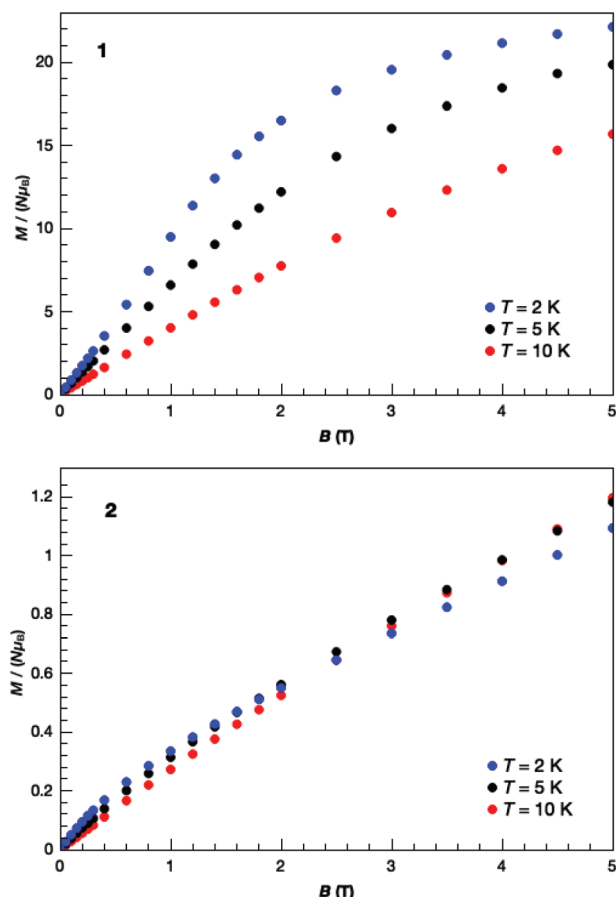
This journal is © the Partner Organisations 2021

Inorg. Chem. Front., 2021, **8**, 1804–1809 | **1807**

Fig. 6 Isothermal molar magnetisation *M versus* applied magnetic field, for **1** (top) and **2** (bottom), collected for *T* = 2, 5 and 10 K, as labelled.

value of ~22.2 μ_B and ~1.1 μ_B for **1** and **2**, respectively. The nuclearity of the two compounds (and the structural complexity of **1**) precludes any quantitative analysis. We note that the magnetic behaviour of the wheel-like complex $[Mn_2^{II}Mn_{14}^{III}(trz)_{14}L_4(\mu_3\text{-}O)_8(H_2O)_{10}](ClO_4)_6$ is also dominated by AF exchange interactions.[17]

Conclusions

The first concerted effort at examining the coordination chemistry of LH$_3$ with Mn has afforded two large and unusual cages: a $[Mn_{16}]$ double square wheel and a $[Mn_{10}]$ contorted square wheel. Both are constructed from corner sharing $[Mn_3O]^{n+}$ triangles dictated by the presence of N,O-chelating L^{3-} and LH^{2-} ligands, which also direct the JT axes of the Mn^{III} ions along the Mn–N(L) bonds. While **1** describes two linked, offset $[Mn_6^{III}Mn_2^{II}]$ wheels, **2** is a single wheel but one in which the upper half is oriented perpendicular to the lower half. Magnetic measurements reveal the presence of strong antiferromagnetic interactions and a diamagnetic ground state in **2** and strong, competing exchange interactions in **1**.

The simplicity of the synthetic procedures that produce **1** and **2** suggests that many more Mn coordination compounds

constructed with LH$_3$ await discovery. Variation in metal salt, oxidation state, base, solvent, co-ligands, temperature and pressure have proved enormously successful in the coordination chemistry of ethanolamine-based ligands with Mn to date.[11–15] Building a library of such species is the first step to understanding what controls the self-assembly process, which, in turn, aids interpretation and exploitation of magneto-structural parameters. We also note that there is no coordination chemistry of this ligand with any other paramagnetic 3d or 4f metal ions. There therefore remains much synthetic chemistry to be explored.

Conflicts of interest

There are no conflicts to declare.

Acknowledgements

Notes and references

1 B. Bleaney and K. D. Bowers, Anomalous paramagnetism of copper acetate, *Proc. R. Soc. London*, 1952, **A214**, 451.

2 K. Kambe, On the paramagnetic susceptibilities of some polynuclear complex salts, *J. Phys. Soc. Jpn.*, 1950, **5**, 48.

3 J. Glerup, D. J. Hodgson and E. Petersen, A novel correlation between magnetism and structural parameters in superexchange coupled chromium(III) dimer, *Acta Chem. Scand.*, 1983, **A37**, 161.

4 H. Weihe and H.-U. Güdel, Angular and distance dependence of the magnetic properties of oxo-bridged iron(III) dimer, *J. Am. Chem. Soc.*, 1997, **119**, 6539.

5 T. Cauchy, E. Ruiz and S. Alvarez, Magnetostructural correlations in polynuclear complexes: The Fe4 butterflies, *J. Am. Chem. Soc.*, 2006, **128**, 15722.

6 A. Caneschi, D. Gatteschi, R. Sessoli, A.-L. Barra, L.-C. Brunel and M. J. Guillot, Alternating current susceptibility, high field magnetization, and millimeter band EPR evidence for a ground S=10 state in $[Mn_{12}O_{12}(CH_3COO)_{16}(H_2O)_4]\cdot2CH_3COOH\cdot4H_2O$, *J. Am. Chem. Soc.*, 1991, **113**, 5873; R. Sessoli, H.-L. Tsai, A. R. Schake, S. Wang, J. B. Vincent, K. Folting, D. Gatteschi, G. Christou and D. N. Hendrickson, High-spin molecules: $[Mn_{12}O_{12}(O_2CR)_{16}(H_2O)_4]$, *J. Am. Chem. Soc.*, 1993, **115**, 1804; R. Sessoli, D. Gatteschi, A. Caneschi and M. A. Novak, Magnetic bistability in a metal-ion cluster,

1808 | *Inorg. Chem. Front.*, 2021, **8**, 1804–1809

This journal is © the Partner Organisations 2021

Nature, 1993, **365**, 141; G. Christou, D. Gatteschi, D. N. Hendrickson and R. Sessoli, Single-molecule magnets, *MRS Bull.*, 2000, **25**, 66.

7 T. Lis, Preparation, structure, and magnetic properties of a dodecanuclear mixed-valence manganese carboxylate, *Acta Crystallogr.*, 1980, **B36**, 2042.

8 J. B. Vincent, C. Christmas, J. C. Huffman, G. Christou, H.-R. Chang and D. N. Hendrickson, Modelling the photo-synthetic water oxidation centre: Synthesis, structure, and magnetic properties of $[Mn_4O_2(OAc)_7(bipy)_2](ClO_4)\cdot 3H_2O$ (bipy=2,2′-Bipyridine), *J. Chem. Soc., Chem. Commun.*, 1987, 236; J. S. Bashkin, H.-R. Chang, W. E. Streib, J. C. Huffman, D. N. Hendrickson and G. Christou, Modelling the photo-synthetic water oxidation center: preparation and physical properties of a tetranuclear oxide bridged Mn complex corresponding to the native S_2 state, *J. Am. Chem. Soc.*, 1987, **109**, 6502.

9 A. J. Tasiopoulos, A. Vinslava, W. Wernsdorfer, K. A. Abboud and G. Christou, Giant single–molecule magnets: A $\{Mn_{84}\}$ torus and its supramolecular nano-tubes, *Angew. Chem., Int. Ed.*, 2004, **116**, 2117.

10 G. Aromí and E. K. Brechin, Synthesis of 3d metallic single-molecule magnets, *Struct. Bonding*, 2006, **122**, 1; C. J. Milios and R. E. P. Winpenny, Cluster-based single-molecule magnets, *Struct. Bonding*, 2014, **164**, 1.

11 M. A. Bolcar, S. M. J. Aubin, K. Folting, D. N. Hendrickson and G. Christou, A new manganese cluster topology capable of yielding high-spin species: Mixed-valence $[Mn_7(OH)_3Cl_3(hmp)_9]^{2+}$ with S ≥ 10, *Chem. Commun.*, 1997, 1485.

12 E. K. Brechin, J. C. Huffman, G. Christou, J. Yoo, M. Nakano and D. N. Hendrickson, A new class of single-molecule magnets: mixed-valent $[Mn_4(O_2CMe)_2(Hpdm)_6][ClO_4]_2$ with an S=8 ground state, *Chem. Commun.*, 1999, 783.

13 K. R. Vignesh, S. K. Langley, B. Moubaraki, K. S. Murray and G. Rajaraman, Large hexadecametallic {MnIII–LnIII} wheels: Synthesis, structural, magnetic, and theoretical characterization, *Chem. – Eur. J.*, 2015, **21**, 16364; A. J. Tasiopoulos and S. P. Perlepes, Diol-type ligands as central 'players' in the chemistry of high-spin molecules and single-molecule magnets, *Dalton Trans.*, 2008, 5537.

14 A. Baniodeh, Y. Lan, G. Novitchi, V. Mereacre, A. Sukhanov, M. Ferbinteanu, V. Voronkova, C. E. Anson and A. K. Powell, Magnetic anisotropy and exchange coupling in a family of isostructural $Fe^{III}_2Ln^{III}_2$ complexes, *Dalton Trans.*, 2013, **42**, 8926.

15 T. N. Hooper, R. Inglis, G. Lorusso, J. Ujma, P. E. Barran, D. Uhrin, J. Schnack, S. Piligkos, M. Evangelisti and E. K. Brechin, Structurally flexible and solution stable $[Ln_4TM_8(OH)_8(L)_8(O_2CR)_8(MeOH)y](ClO_4)_4$: A playground for magnetic refrigeration, *Inorg. Chem.*, 2016, **55**, 10535.

16 M. V. Baker, D. H. Brown, B. W. Skelton and A. H. White, Chromium complexes of hydroxyl-functionalised 1,3,5-tria-zacyclohexanes, *J. Chem. Soc., Dalton Trans.*, 1999, 1483.

17 M. Riaz, R. K. Gupta, H.-F. Su, Z. Jagličić, M. Kurmoo, C.-H. Tung, D. Sun and L.-S. Zheng, Hexadecanuclear $Mn^{II}_2Mn^{III}_{14}$ molecular torus built from in situ tandem ligand transformations, *Inorg. Chem.*, 2019, **58**, 14331.

18 O. V. Dolomanov, L. J. Bourhis, R. J. Gildea, J. A. K. Howard and H. Puschmann, OLEX2: a complete structure solution, refine-ment and analysis program, *J. Appl. Crystallogr.*, 2009, **42**, 339.

19 G. M. Sheldrick, SHELXT – Integrated space-group and crystal-structure determination, *Acta Crystallogr., Sect. A: Found. Adv.*, 2015, **A71**, 3.

20 G. M. Sheldrick, Crystal structure refinement with SHELXL, *Acta Crystallogr., Sect. C: Struct. Chem.*, 2015, **C71**, 3.

21 P. Comar, T. Rajeshkumar, G. S. Nichol, M. B. Pitak, S. J. Coles, G. Rajaraman and E. K. Brechin, Switching the orientation of Jahn–Teller axes in oxime-based MnIII dimers and its effect upon magnetic exchange: a combined experimental and theoretical study, *Dalton Trans.*, 2015, **44**, 19805; W. P. Barros, R. Inglis, G. S. Nichol, T. Rajeshkumar, G. Rajaraman, S. Piligkos, H. O. Stumpf and E. K. Brechin, From antiferromagnetic to ferro-magnetic exchange in a family of oxime-based MnIII dimers: a magneto-structural study, *Dalton Trans.*, 2013, **42**, 16510; N. Berg, T. Rajeshkumar, S. M. Taylor, E. K. Brechin, G. Rajaraman and L. F. Jones, What Controls the magnetic interaction in bis–μ–alkoxo MnIII dimers? A combined experimental and theoretical exploration, *Chem. – Eur. J.*, 2012, **18**, 5906.

This journal is © the Partner Organisations 2021

Inorg. Chem. Front., 2021, **8**, 1804–1809 | **1809**